Numerical models of Rayleigh-Taylor instabilities superimposed upon convection

HARRO SCHMELING

Schmeling, H. 1988 12 30: Numerical models of Rayleigh-Taylor instabilities superimposed upon convection. *Bulletin of the Geological Institutions of the University of Uppsala,* N.S. Vol. 14, pp. 95–109. Uppsala ISSN 0302-2749.

Gravity driven instabilities in the earth's crust are caused by inverted density distributions which may be of combined compositional and thermal (convective) origin. An order of magnitude estimate suggests that such instabilities may develop in the lower crust of thermally anomalous regions if the effective viscosity is less than $10^{18}-10^{19}$ Pa s. To compare the vigour of compositionally driven gravity overturns with convection instabilities, and to describe their effect on the temperature field, a nondimensional number Rt ("Rayleigh-Taylor number.") is defined, which is analogous to the Rayleigh number, Ra, used for convection. Rt, multiplied by a factor depending on the geometrical arrangement, C, describes the diapiric heat advection relative to conduction (i.e. Rt C is a diapiric Peclet no.). Numerical models are presented in which convective instabilities are superimposed upon compositional (Rayleigh-Taylor) instabilities. Ra-Rt-space is explored up to Ra = 30 000 and Rt = 10 000. Several flow regimes are identified, in general agreement with previous results based on linear stability analysis; after one Rayleigh-Taylor overturn the flow may become stable, it may oscillate or it may continue to convect in either one or two layers separated by an irregular oblique interface. In the case of compositional density contrasts only, Rt gives a good measure for the distortion of the temperature field or the anomalous heat flow: diapiric advection of heat becomes significant for Rt of a few hundred or more. Heat flow anomalies associated with diapirism may be interpreted in terms of Rt which contains information about the effective viscosity.

H. Schmeling, The Hans Ramberg Tectonic Laboratory, Institute of Geology, Uppsala University, Box 555, S-751 22 Uppsala, Sweden. *Received 24th April 1987; revision received 20th November 1987.*

Introduction

Gravity driven flows are quite common within the earth (Ramberg, 1981). If the driving buoyancy forces are due to compositional density differences, the flows fall into the class of diapirism. Rayleigh-Taylor (R.T.) instabilities arising from an inverse density stratification are a major subdivision of this class of flows (Ramberg, 1981). Thermally induced density differences are responsible for flows known as thermal convection. Both of these general flow types have been studied in great detail in connection with salt tectonics (R.T.), plutonism (R.T.), plate tectonics and mantle flows (convection) (see e.g. Woidt, 1978, Schmeling and Jacoby, 1981, Marsh, 1982, Christensen, 1984a, Jackson and Talbot, 1986, Schmeling, 1987, Schmeling et al., 1987). Studies in which both compositional and thermal density differences are considered simultaneously are rare. Convection in a compositionally layered mantle was investigated by Richter and Johnson (1974), Christensen and Yuen (1984), Christensen (1984b) and others, but in these studies the density stratification was such as to stabilize the flow. Recently, Neugebauer and Reuther (1986) studied the rise of diapiric volumes with inverted density by simultaneously solving the equation of momentum and heat transfer.

Two questions arise if one considers a combination of a R.T. – and a convective instability. Firstly, how do the buoyancy effects arising from compositional and thermal origin superimpose dynamically? This question involves the transition from one R.T.-overturn to multiple convective overturns. Secondly, how is the temperature field affected? This question might even be important for a pure R.T.-overturn, which disturbs the temperature field, but in which thermally induced buoyancy plays a minor role.

There are two environments in which the above mentioned questions might be important. In tectonically active continental regions, subjected to anomalously high heat flow from the mantle, elevated temperatures and wet conditions (inferred from high

electrical conductivities, R. Hutton, 1987, pers. comm.) might lower effective viscosities of the ductile lower crust (see e.g. Kirby, 1983, for a compilation of crustal rheologies). If these are sufficiently low, thermal convection may be possible, and can be assessed by the Rayleigh number Ra. Ra controls the vigour of convection and must be larger than a critical value (which is of the order 1000). The Rayleigh number is defined as

$$Ra = \frac{\varrho g \alpha \beta h^4}{\varkappa \eta} = \frac{\varrho g \alpha \Delta T h^3}{\varkappa \eta} \qquad (1)$$

For the definition of these and further quantities occurring below, see Table 1. Taking tentatively $\varrho = 2800\ kgm^{-3}$, $g = 10\ ms^{-2}$, $\alpha = 2.4 \cdot 10^{-5}\ K^{-1}$, $\beta = 0.03\ K\ m^{-1}$, $h = 15$ km, $\varkappa = 10^{-6}\ m^2\ s^{-1}$, a viscosity as low as 10^{18} Pa · s is required to give an overcritical Rayleigh number. In such environments, any diapirism or R.T.-instability (e.g. due to partial melting within the lower crust) will be strongly influenced by thermally induced buoyancy effects. Note that the above assessment is only an order of magnitude estimate, since the actual viscosity is strongly temperature and stress dependent. To account for the temperature dependence, η in (1) should represent the viscosity at the mean temperature of the convecting layer (Stengel et al., 1982).

If the rise of a diapir (e.g. of salt or granite) is only associated with a R.T.-instability (i.e. Ra is too small for convection), the distortion of isotherms during rise might still be significant, thereby changing the total heat flow. As will be shown below, this effect can be assessed by a single, nondimensional number, introduced here as the Rayleigh-Taylor number.

Table 1. List of quantities. Primed quantities are nondimensional according to equations 7 and 8.

Quantity	Meaning	Equation
u.C	Geometry factor	3
g	Gravity acceleration	1
h	Total thickness of the layer	1
Pe	Peclet number	4
q	Surface heat flow, averaged over the box	
q_o	Initial value of q	
Ra	Rayleigh number	1
Ra_c	Critical Rayleigh number	
Rt	"Rayleigh-Taylor"-number	2
t	Time	
T	Temperature field	5,6
ΔT	Temperature difference between top and bottom of the convecting layer	1
u	Horizontal flow velocity	6
u_{max}	Maximum value of u	
u_{ch}	Characteristic velocity of the flow	3
$\bar{v}$	Flow velocity vector field	9
$\bar{v}_o$	$\bar{v}$ at time t=0	9
w	Vertical flow velocity	6
w_{max}	Maximum value of w	
x	Horizontal coordinate	5
z	Vertical coordinate	5
α	Thermal expansivity	1
β	Temperature gradient	1
γ	Growth rate of a perturbation	8,9
Γ	Two dimensional unit step function (=0 at positions, occupied by light material, else=1)	5
η	Dynamic viscosity	1
$\varkappa$	Thermal diffusivity	1
ψ	Stream function	5
ψ_{max}	Maximum value of ψ	
ϱ	Density	1
$\Delta\varrho$	Density contrast at the interface	2

R.T.-instabilities superimposed upon convection

The Rayleigh-Taylor number

Thermal convection is only possible if Ra exceeds the critical Rayleigh number Ra_c. For overcritical Ra, the dynamical and thermal behaviour of convection is a strong function of Ra. In contrast, a R.T.-instability in viscous fluids occurs for any inverted density stratification, regardless of how small the density contrast is. For a two layer R.T.-instability with constant viscosity and a density contrast $\Delta\varrho$ small compared to ϱ, the density contrast reduces merely to a scaling property. This implies that overturns with different $\Delta\varrho$ are dynamically similar (Weijermars and Schmeling, 1986). However, their effect on the temperature field depends on $\Delta\varrho$, β, K etc., implying that dynamically similar R.T.-overturns generally will not be thermally similar. Of course, for a temperature dependent viscosity, even dynamic similarity breaks down for different temperature fields.

To compare R.T.-overturns with thermal convection and to describe the effect on the temperature field, it is therefore appropriate to introduce a nondimensional number, subsequently called the Rayleigh-Taylor number:

$$Rt = \frac{\Delta\varrho g h^3}{\varkappa \eta} \qquad (2)$$

It can be shown (using e.g. equations (5), (6), (7) below) that pure R.T.-overturns having the same boundary and initial conditions and a constant viscosity will be dynamically *and* thermally similar if they have the same Rt.

Obviously Rt can be constructed from Ra by replacing the thermally induced density contrast

$\varrho\alpha\Delta T$ in Ra by the compositional density contrast $\Delta\varrho$. Rt has been previously referred to in the literature as the boundary Rayleigh number (Richter and Johnson, 1974; Christensen and Yuen, 1984) for layered convection problems. In the present study, however, it is a measure of the vigour of a R.T.-instability and its potential to advect heat. The latter property can be seen by defining the characteristic velocity of a R.T.-overturn by

$$u_{ch} = C \frac{\Delta\varrho g h^2}{\eta} \tag{3}$$

where C is a factor depending on the geometrical arrangement. Using this velocity for the Peclet number, which is a measure of the ratio of heat advection to conduction, it turns out

$$Pe = \frac{u_{ch}\, h}{\varkappa} = C \cdot Rt \tag{4}$$

Thus, Rt is a sort of Peclet number of a R.T.-overturn.

Method

Numerical simulation of convection plus R.T.-instability is carried out by solving the coupled equations of motion and heat transport in two dimensions in a rectangular box (see e.g. Christensen 1984a, b):

$$\nabla^4\psi' = Ra \frac{\partial T'}{\partial x'} - Rt \frac{\partial \Gamma}{\partial x'} \tag{5}$$

$$\frac{\partial T'}{\partial t'} = \nabla^2 T' - u' \frac{\partial T'}{\partial x'} - w' \frac{\partial T'}{\partial z'} \tag{6}$$

For the definition of these variables, see Table 1. The primes indicate nondimensional quantities. For dimensionalisation, one has to use:

$$\begin{aligned} \psi &= \varkappa \cdot \psi' \\ T &= \Delta T \cdot T' \\ (x,z) &= h \cdot (x',z') \\ t &= \frac{h^2}{\varkappa} \cdot t' \\ (u,w) &= \frac{\varkappa}{h}(u',w') \end{aligned} \tag{7}$$

The function Γ (x', z') is a two dimensional, unit step function jumping from 0 to 1 at the position of the interface between the heavy and light material. The equations are solved with a Finite Element Code developed by Christensen (1984a, b) and Christensen and Yuen (1984). Unless specified otherwise, the boundary conditions at the top and bottom are free slip with constant temperature, and the side walls are reflective. Viscosity is constant and the same within the two fluids. In large scale natural examples, of course, viscosity would actually vary with depth in response to the geothermal gradient. The interface is situated initially at half depth. Initial perturbations are applied on both the temperature field and the interface. The aspect ratio is $\sqrt{2}$.

Models

In the first set of models, Ra and Rt are varied simultaneously to cover the transition from pure convection (Rt=0) to a pure R.T.-instability (Ra=0). Ra, Rt combinations are chosen in a way to give approximately the same nondimensional growth rate

$$\gamma' = \frac{h^2}{\varkappa} \cdot \gamma \tag{8}$$

where γ is the dimensional growth rate describing the amplitude of the velocity field during early time stages

$$\vec{v} = \vec{v}_0 \exp(\gamma t) \tag{9}$$

The scaling of γ in isothermal R.T.-instabilities (Schmeling, 1987, see also Ramberg, 1981) differs from (8) by the factor Rt. The Ra, Rt values chosen

Table 2: Parameters of numerical models (see also Fig. 1)

Model no.	Ra	Rt	Regime
1	0	1276.7	R.T.
2	657.5	1276.7	R.T.
3	1315.0	957.5	R.T.
4	1972.5	638.4	OSCILL.
5	2301.1	478.8	CONV.
6	2630.0	319.2	CONV.
7	2958.8	159.6	CONV.
8	3287.5	0	CONV.
9	0	10	R.T.
10	0	100	R.T.
11	0	1000	R.T.
12	0	10000	R.T.
13	10000	10000	R.T. → 2 LAYER CONV.
14	20000	10000	R.T. → 2 LAYER CONV.
15	30000	10000	R.T. → 2 LAYER CONV. → → 1 LAYER CONV.

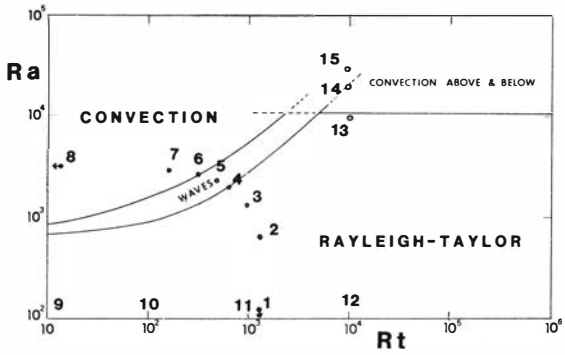

Fig. 1. (Modified from Richter and Johnson, 1974). Ra, Rt-space for a two-layer system with an inverse density stratification heated from below. The space is subdivided into regimes of a single R.T.-overturn ("Rayleigh-Taylor"), whole layer convection ("convection", mixing the two sublayers), convection below and above the interface after one R.T.-overturn, and oscillatory behaviour with a wobbling interface after one overturn ("waves"). The Ra, Rt combinations of the numerical models are indicated.

(models 1 to 8) should result in a growth rate $\gamma' \cong 60$, as can be determined from linear stability analysis, and are shown in Fig. 1 (see also Table 2 for a summary of models).

Fig. 1 was taken from Richter and Johnson (1974), who carried out a linear stability analysis for a two layer system with a stabilizing density contrast (heavy material below), other conditions being the same as in the present models. They found that the region now labeled "Rayleigh-Taylor" was stable, that convection is possible in the "Convection" regime, while above the horizontal line convection occurs above and below the interface. In the transitional regime "waves" they predicted oscillatory behaviour (i.e. a wobbling interface without overturning).

Fig. 2 shows the maximum stream function ψ'_{max} of the models 1 to 8 with time. ψ'_{max} is a measure of the velocity amplitude ($u'_{max} \cong \pi \cdot \psi'_{max}$, $w'_{max} \cong \pi \cdot \psi'_{max}/\sqrt{2}$), where u'_{max}, w'_{max} are the maximum horizontal and vertical velocity, respectively. For model 1, Rt=1277, Ra=0, while model 2 had the same Rt but Ra=657.4 ($=Ra_c$). Without Rayleigh-Taylor instability, both Ra=0 and Ra=Ra_c would show the same behaviour (no motion). However, in combination with a R.T.-instability, Ra=Ra_c leads to a considerably more vigorous overturn. Increasing the relative importance of convection (model 3) does not show a significant change in the overturn behaviour. However, for Ra, Rt-combinations reaching the transition zone toward convection (model 4), oscillatory behaviour is observed after the first overturn (as predicted by Richter and Johnson, 1974). The run was actually continued until t'=1.6 and did not show significant changes in the shapes and amplitudes of the oscillations. The inset diagram shows the oscillatory behaviour if one starts with a stably stratified situation (which is then perturbed at t'=0). For models 5 to 7 continuous heat input after the first R.T.-overturn is so strong that the circulation continues, showing damped oscillations which seem to converge toward a steady state after complete mixing. Model 8 shows the time behaviour of pure convection (Rt=0).

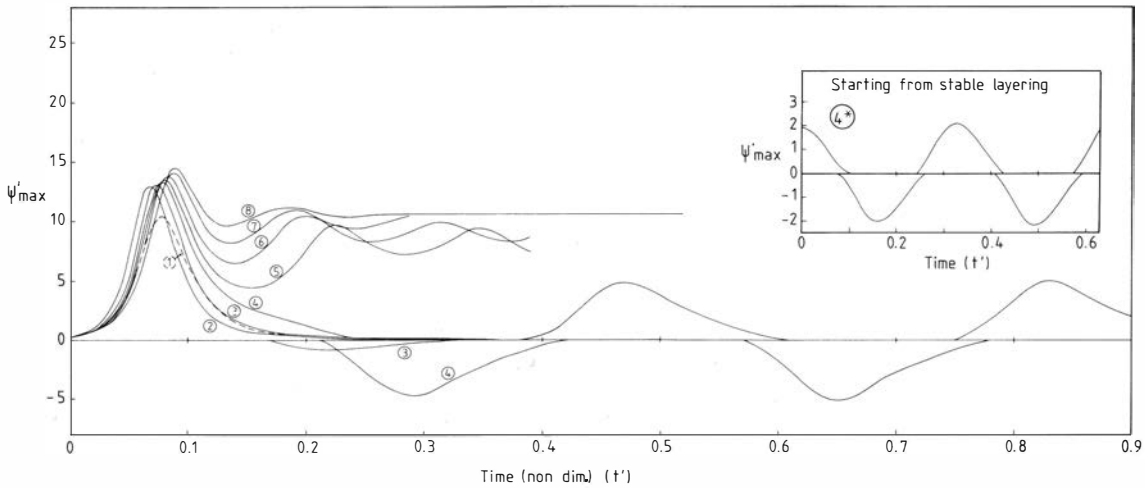

Fig. 2. Maximum nondimensional stream function (~ vigour of the flow), as a function of time, for the models 1 to 8. Note the single overturn behaviour for models 1–3, the oscillations of model 4 and the multiple overturn convection of models 5–8. The inset diagram shows model 4, if started with a perturbed interface between heavy material below and light material above.

a) Model1

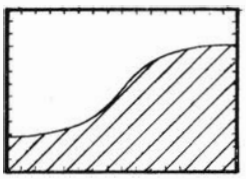

Time= 0.0620

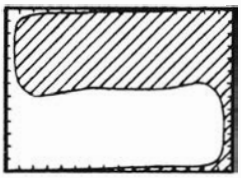

Time= 0.154

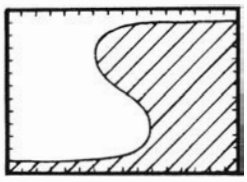

Time= 0.0820

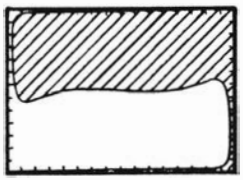

Time= 0.234

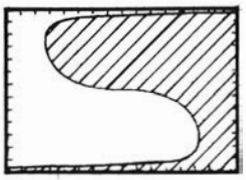

Time= 0.102

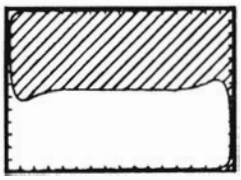

Time= 0.314

Fig. 3a–e. The evaluation of the interface of models 1, 3, 4, 5 and 8, respectively. The lighter, hatched material was initially situated in the lower half of the models. The times (t') are nondimensional. The (Ra, Rt) values of the models are: 1:(0; 1276.7), 3: (1315; 975.5), 4:(1972.5; 638.4), 5:(2301.1; 478.8), 8:(3287.5; 0).

b) Model 3

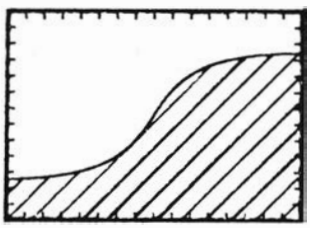

Time= 0.0600

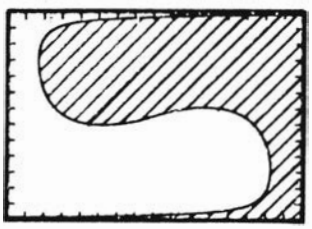

Time= 0.0980

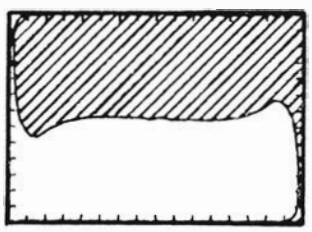

Time= 0.298

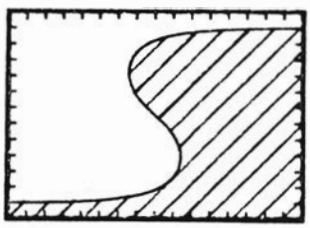

Time= 0.0730

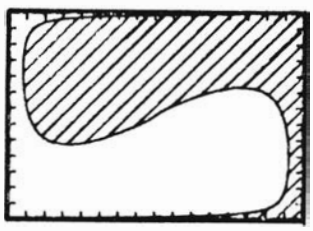

Time= 0.118

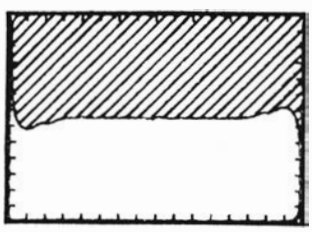

Time= 0.458

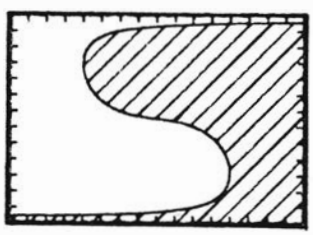

Time= 0.0830

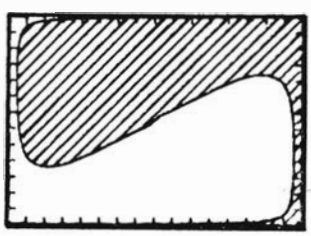

Time= 0.154

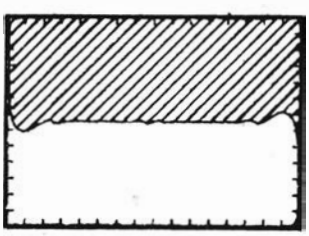

Time= 0.618

c) Model 4

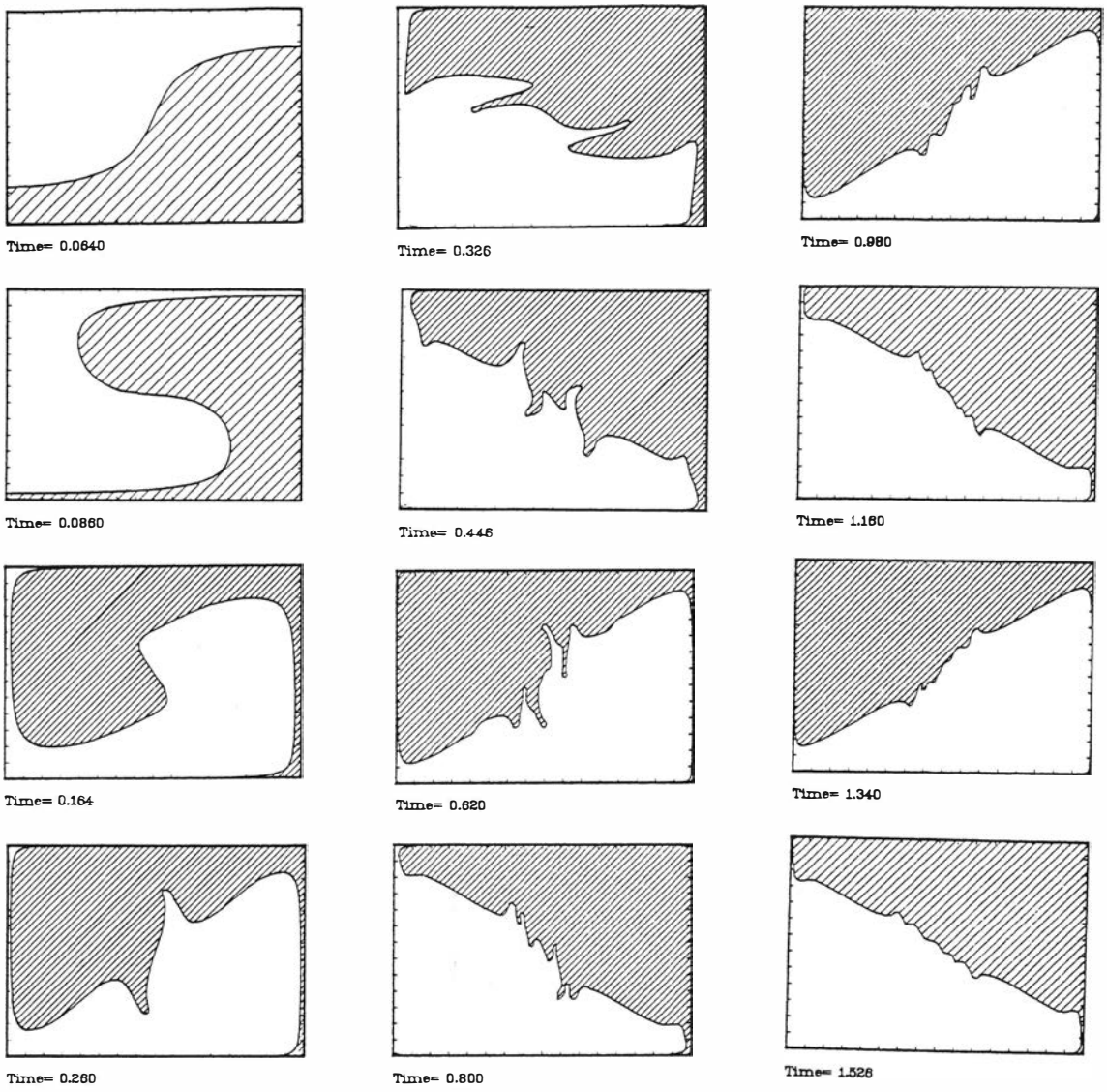

Figure 3 continued.

Some of the models 1 to 8 are shown in Fig. 3a–3e. The lighter material, which was initially in the lower part of the box, is hatched. Models 1 and 2 (Fig. 3a and b) show just one overturn, with an increasing tendency towards overshooting (Fig. 3b, t'=0.154). Fig. 3c shows the overturn and subsequent oscillation of model 4. Note the decrease in amplitude of the irregularities which formed at the time t'=0.26. This decrease is due to a stable density stratification after the R.T.-overturn. In model 5 (Fig. 3d), the overshoot after one overturn is so strong that the material continues to circulate. The increasing degree of mixing becomes evident. Note that Richter and Johnson (1974) still predict oscillating waves for this Ra, Rt combination and aspect ratio. The difference is presumably due to the fact that here the model started with an unstable, inverted density statification. This leads to diapiric stems after one overturn, which continue to drive the flow (Fig. 3d, t'=0.117). With decreasing influ-

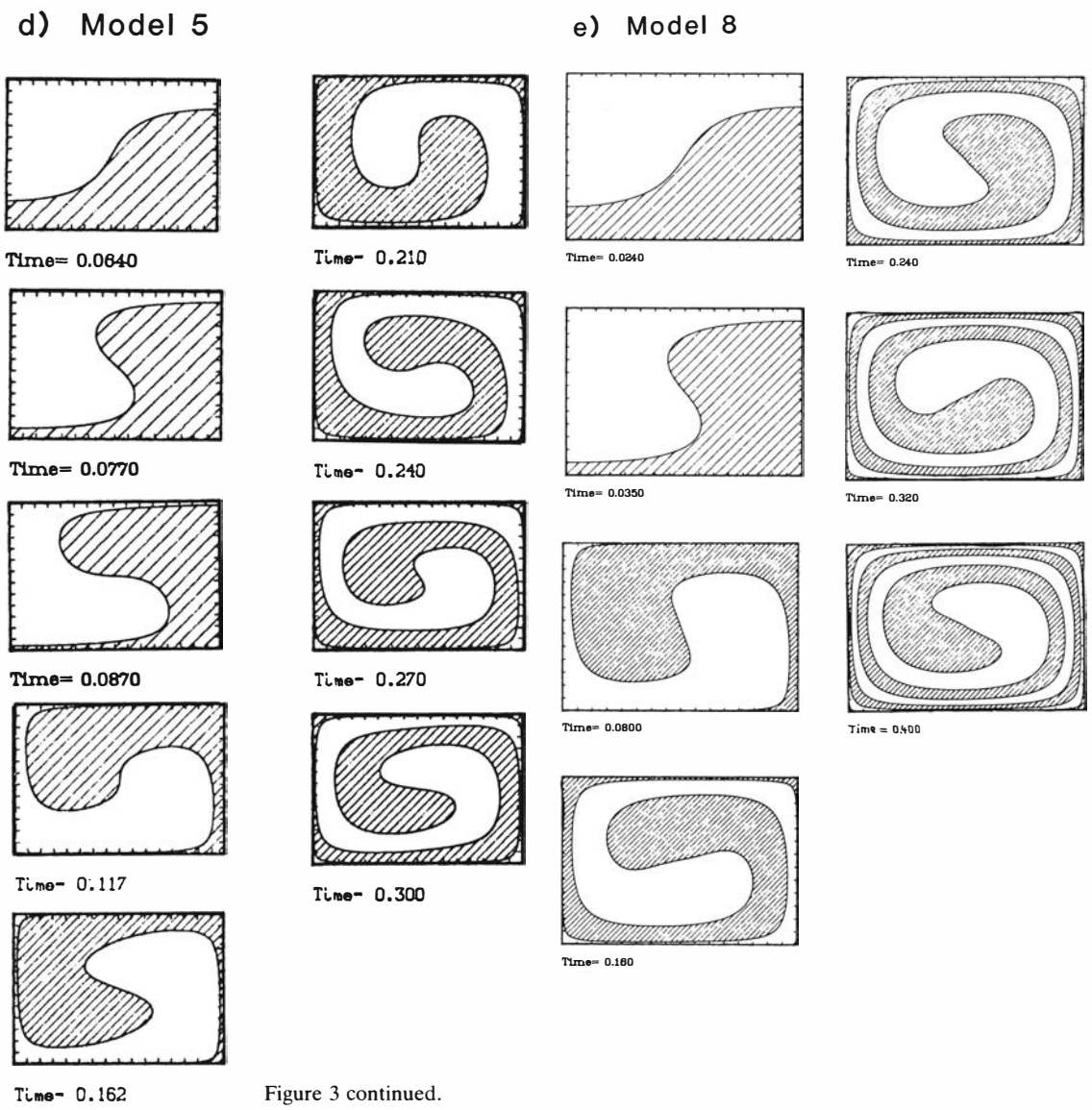

Figure 3 continued.

ence of Rt, mixing becomes more efficient (see Fig. 3e with Rt=0, where the interface represents only a passive marker line).

For the oscillatory wobbling case (model 4 or 4* in Fig. 2 or 3c), the isotherms and streamlines are shown in Fig. 4 for approximately one oscillation. The driving mechanism of this oscillation can be described as follows. Fig. 4a: The distorted interface moves toward mechanical equilibrium; Fig. 4b: the isotherms are distorted by this movement which leads to thermal destabilization and overshoot of the interface: Fig. 4c: due to the distorted interface, motion slows down and reverses to level out the isotherms; Fig. 4d, e show the later reversed version of this process.

In the following series of models (numbers 9 to 12), the Rayleigh number was set to zero, while increasing Rt from 10 to 10 000. Figs. 5a to d show the evolution of temperature during and after a R.T.-overturn, together with the streamlines and the interface. For Rt=10 and 100 (Figs. 5a and b), the temperature field remains almost undisturbed, i.e. heat diffusion effectively compensates heat advection during diapirism. For Rt=1 000 and 10 000 (Figs. 5c and d), significant advection takes place, because the diapir transports heat. The

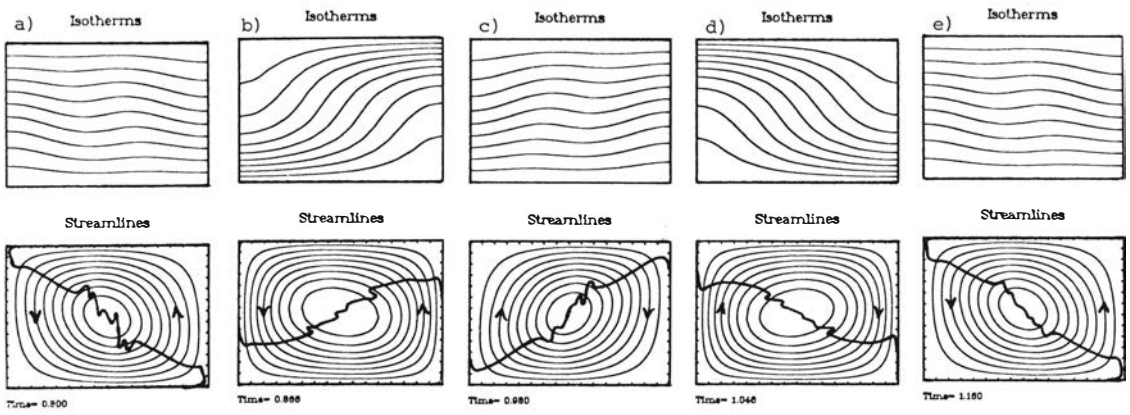

Fig. 4. Isotherms (top series), streamlines and interface (bottom series) of model 4 during approximately one oscillation. The indicated times are nondimensional. The visible interface separates light material above from heavy material below.

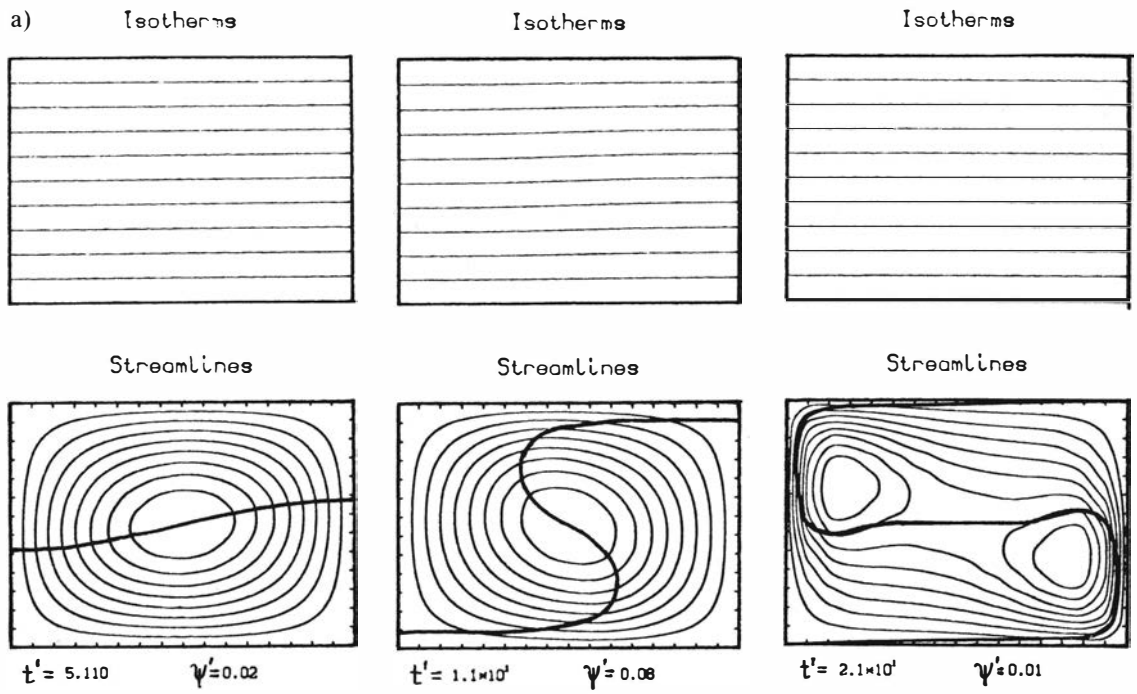

Fig. 5. Evolution of the temperature field (top of figures) during one R.T.-overturn. Ra=0, Rt is 10 (Fig. 5a), 100 (Fig. 5b), 1000 (Fig. 5c), 10 000 (Fig. 5d). Times are nondimensional. Note that the number of streamlines is scaled by the maximum stream function ψ' at any stage, and that the flow velocities at the late stages in each figure are very small.

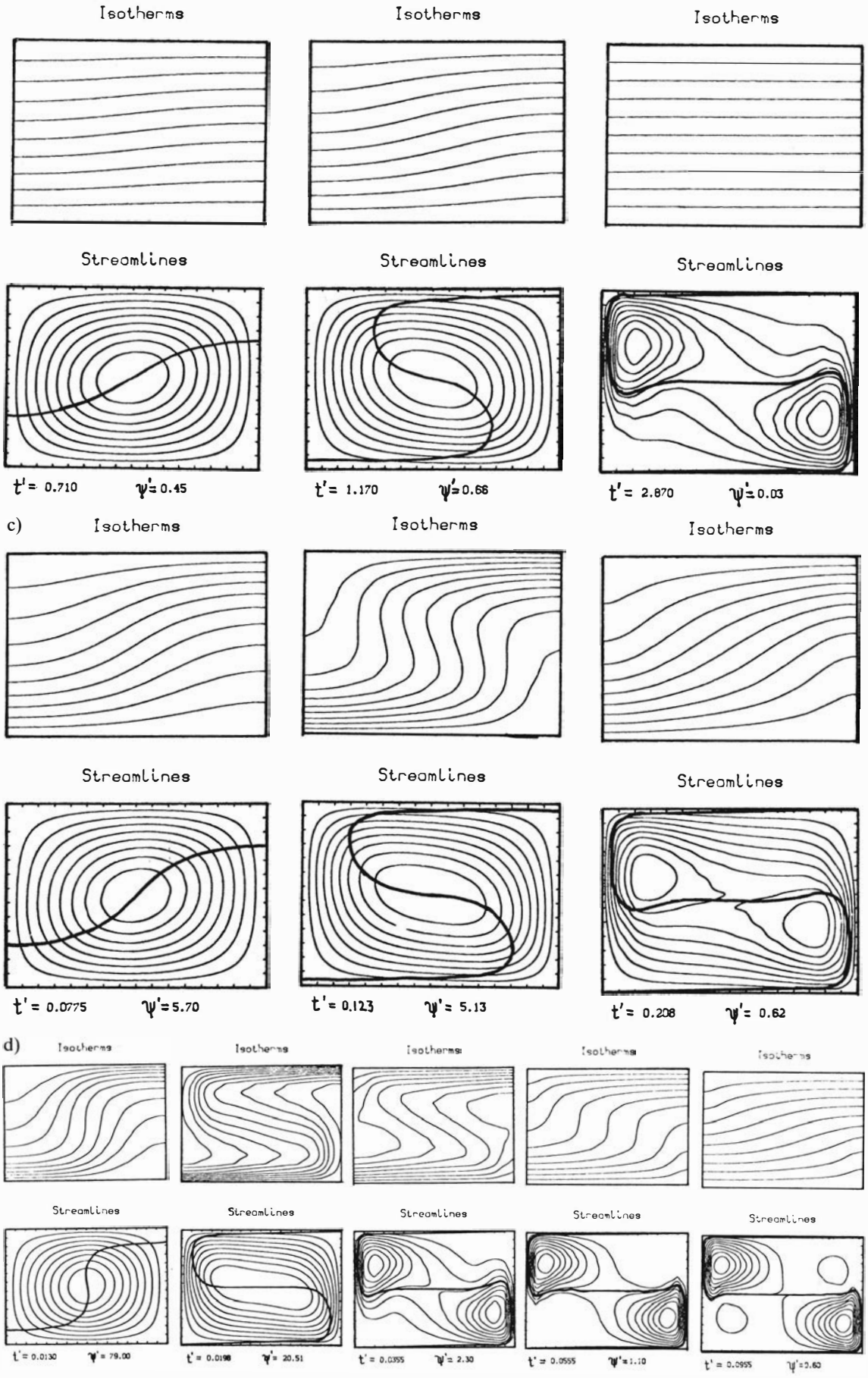
Isotherms
Isotherms
Isotherms
Streamlines
Streamlines
Streamlines
t'= 0.710 ψ'= 0.45
t'= 1.170 ψ'= 0.66
t'= 2.870 ψ'= 0.03
c)
Isotherms
Isotherms
Isotherms
Streamlines
Streamlines
Streamlines
t'= 0.0775 ψ'= 5.70
t'= 0.123 ψ'= 5.13
t'= 0.208 ψ'= 0.62
d)
Isotherms
Isotherms
Isotherms
Isotherms
Isotherms
Streamlines
Streamlines
Streamlines
Streamlines
Streamlines
t'= 0.0130 ψ'= 79.00
t'= 0.0198 ψ'= 20.51
t'= 0.0355 ψ'= 2.30
t'= 0.0555 ψ'= 1.10
t'= 0.0955 ψ'= 0.60

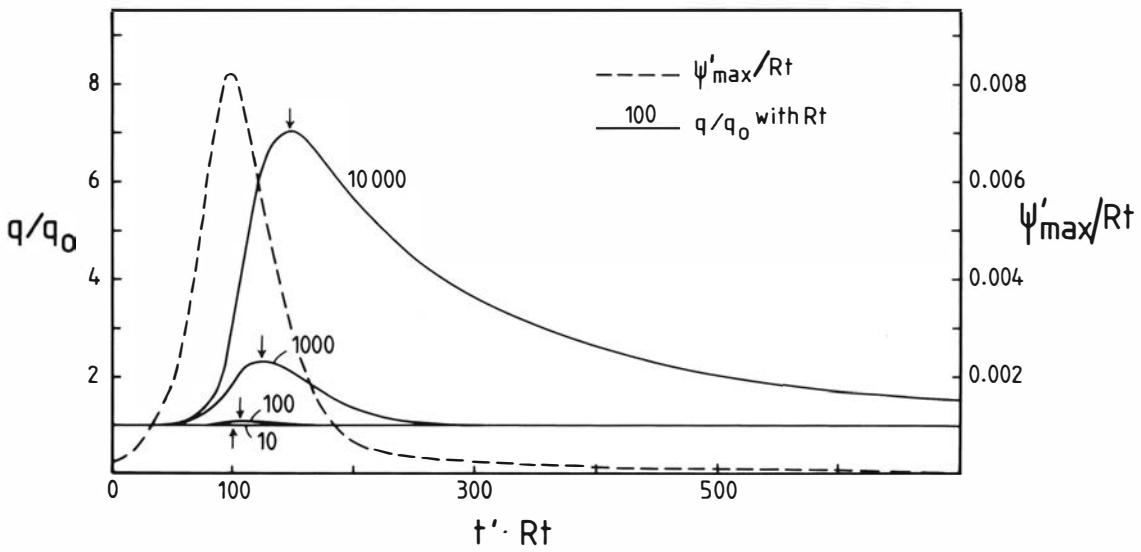

Fig. 6. Maximum stream function ψ'_{max}/Rt (right scale) and mean relative surface heat flow (left scale) as a function of nondimensional time for the models 9 to 12. Ra=0 and Rt changes from 10 to 10 000.

change with time of the mean surface heat flow induced by a R.T.-overturn (with Ra=0) is shown in Fig. 6 for the previous models. The dashed curve gives a maximum nondimensional stream function, which becomes the same for all models if multiplied by Rt (R.T.-overturns with different Rt are dynamically similar). The maximum of this curve indicates the most vigorous stage during an overturn. The surface heat flow q is averaged over the box and divided by the initial heatflux q_o. For Rt=10 and 100 no significant change in q/q_o is observed. For Rt=1 000 or 10 000, q increases significantly, showing a time lag with respect to the maximum overturn velocity (i.e. ψ'_{max}) and an increased recovery time back to q_o.

The behaviour near the triple point between one Rayleigh-Taylor overturn, single- and double layer convection (Fig. 1) is indicated by the models 13 to 15 (Figs. 7a to c). While model 13 (Fig. 7a), with Ra=Rt=10 000, effectively becomes stable after one overturn (note that the streamline spacing is scaled by ψ'_{max} which decreases drastically during the run), model 14 (Fig. 7b) develops two (weak) convection cells, one on either side of an oblique, weakly oscillating interface. If Ra is increased to 30 000, a strong R.T.- (+ convective) overturn oc-

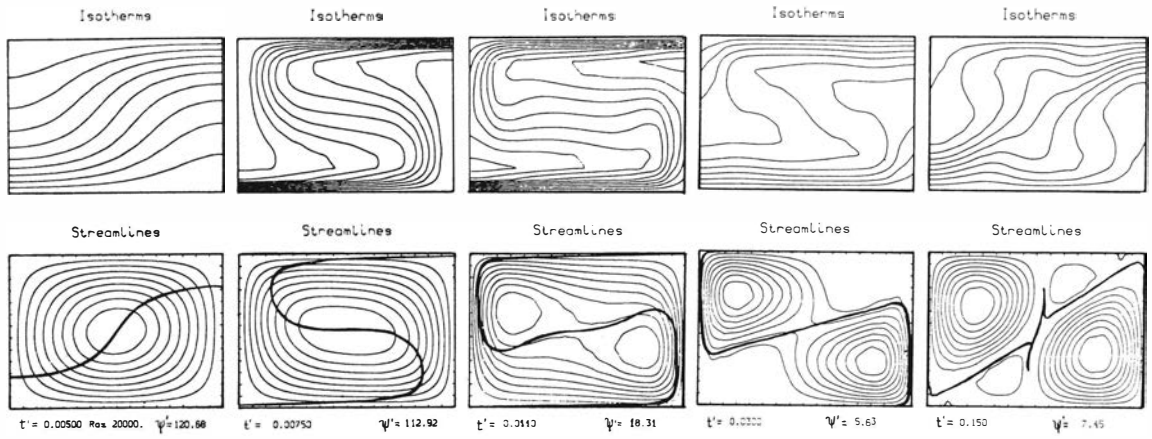

Fig. 7. Evolution of temperature, streamlines and interface of the models 13 (Fig. 7a), 14 (Fig. 7b) and 15 (Fig. 7c). They show the transition from an R.T.-overturn (a), to two-layer convection (b) and one-layer convection (c).

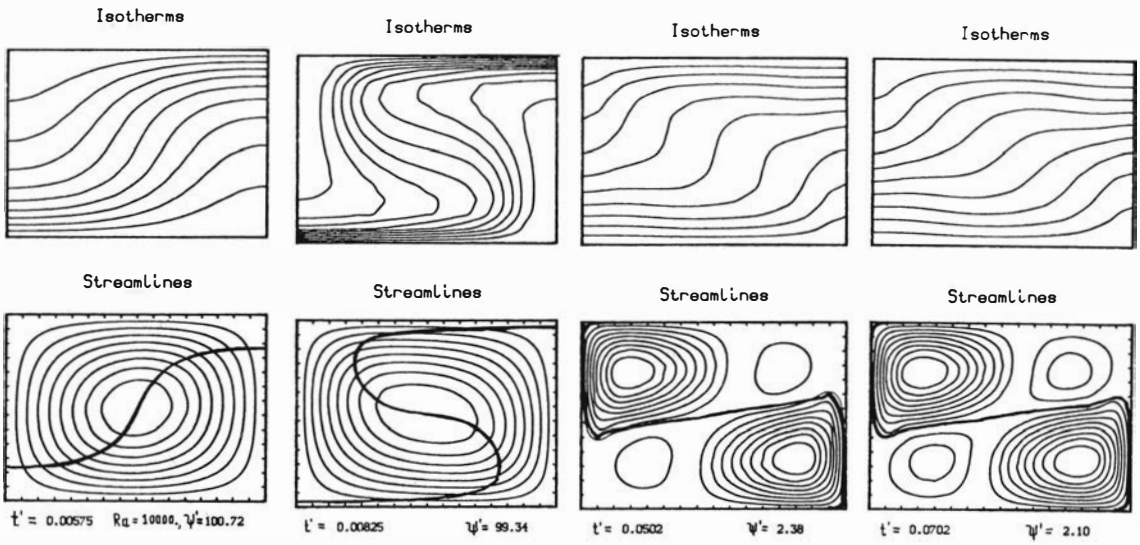
Isotherms
Isotherms
Isotherms
Isotherms
Streamlines
Streamlines
Streamlines
Streamlines
t'= 0.00575 Ra = 10000., ψ'=100.72
t'= 0.00825 ψ'= 99.34
t'= 0.0502 ψ'= 2.38
t'= 0.0702 ψ'= 2.10

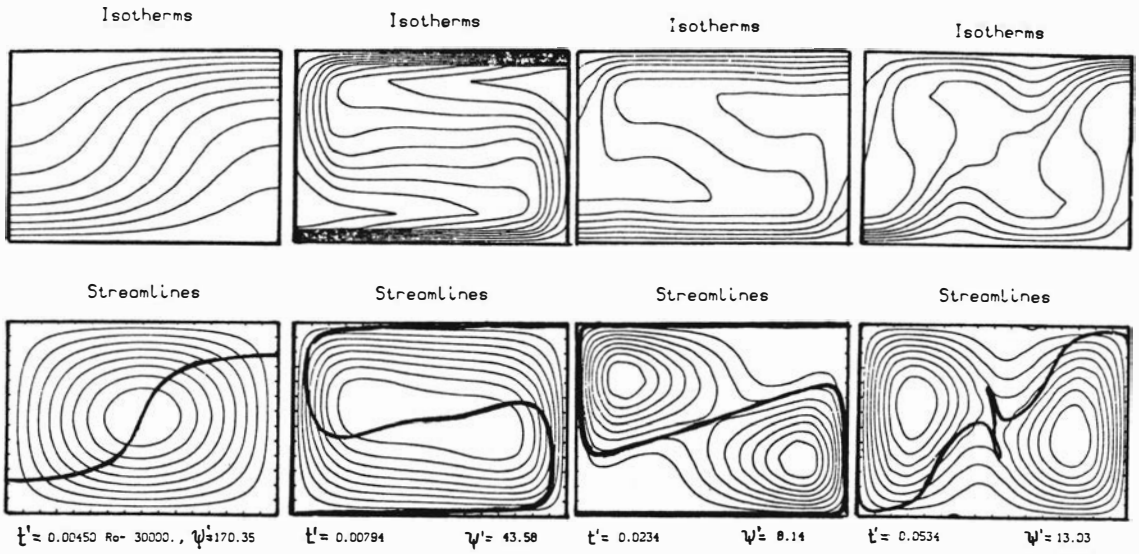
Isotherms
Isotherms
Isotherms
Isotherms
Streamlines
Streamlines
Streamlines
Streamlines
t'= 0.00450 Ra= 30000., ψ'=170.35
t'= 0.00794 ψ'= 43.58
t'= 0.0234 ψ'= 8.14
t'= 0.0534 ψ'= 13.03

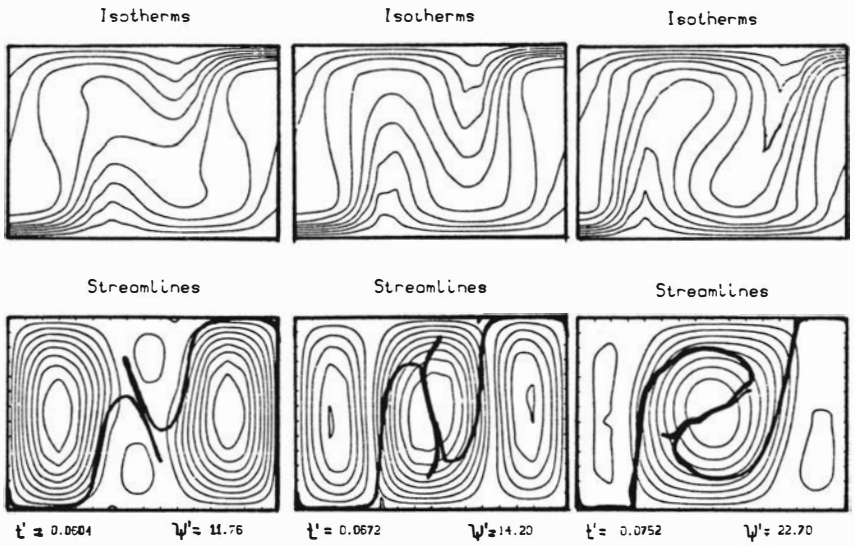
Isotherms
Isotherms
Isotherms
Streamlines
Streamlines
Streamlines
t'= 0.0604 ψ'= 11.76
t'= 0.0672 ψ'=14.20
t'= 0.0752 ψ'= 22.70

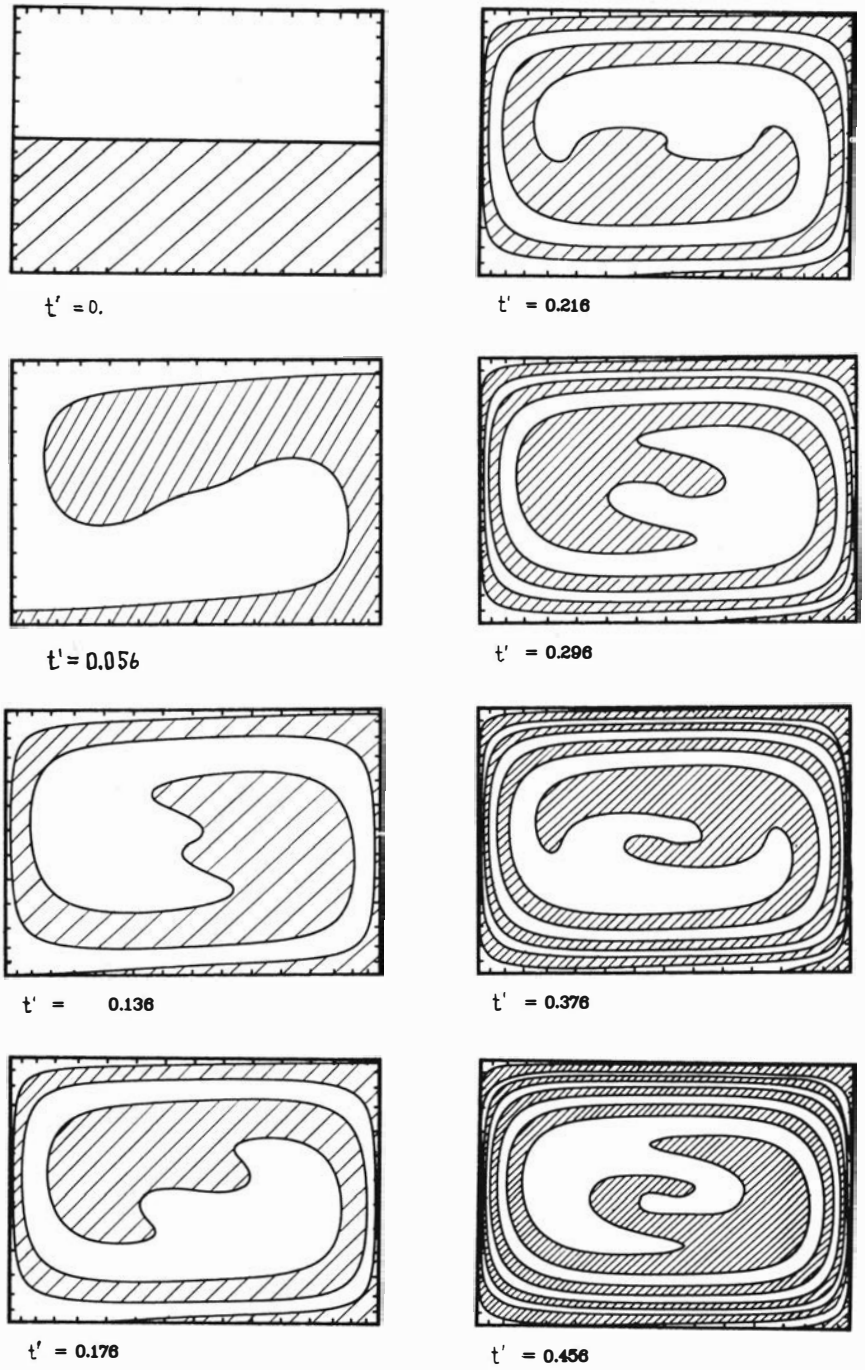

Fig. 8. Convection with Ra= 10 000 and no-slip boundary conditions at top and bottom. The interface between the hatched and white region is passively driven by the convective flow (Rt=0).

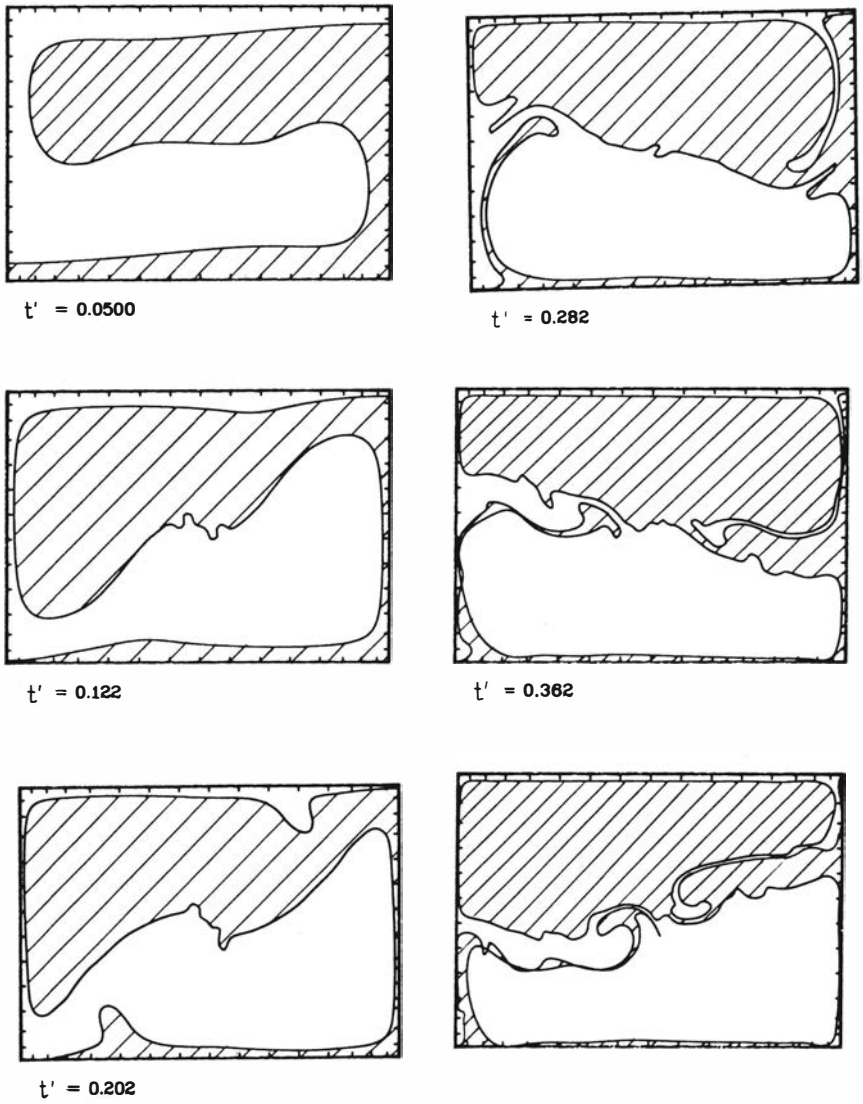

Fig. 9. Model with Ra=7 500, Rt=2 500 and no-slip condition at top and bottom. Note that the lighter hatched material was originally situated in the lower half.

curs (Fig. 7c), followed by two separated convection cells on either side of the strongly distorted interface. However, these two cells are not stable. Instead a third cell develops which contains the interface, takes over the main flow and will eventually lead to one-layer convection and complete mixing (Fig. 7c).

Discussion

Transition from one to multiple overturns

The above models give a general view of Rayleigh-Taylor instabilities superimposed upon thermal convection as well as the effect of one R.T.-overturn on the temperature field. The Ra, Rt space is explored up to Ra, Rt values of 30 000 and 10 000, respectively.

The transition from one R.T.-overturn to multiple convection overturns is found to coincide with the regime of marginal stability for the case of a stabilizing density stratification (see Fig. 1). The overstable oscillatory mode near this marginal stability regime found by linear stability analysis (Richter and Johnson, 1974) occurred also in the present models. Starting with an unstable stratifi-

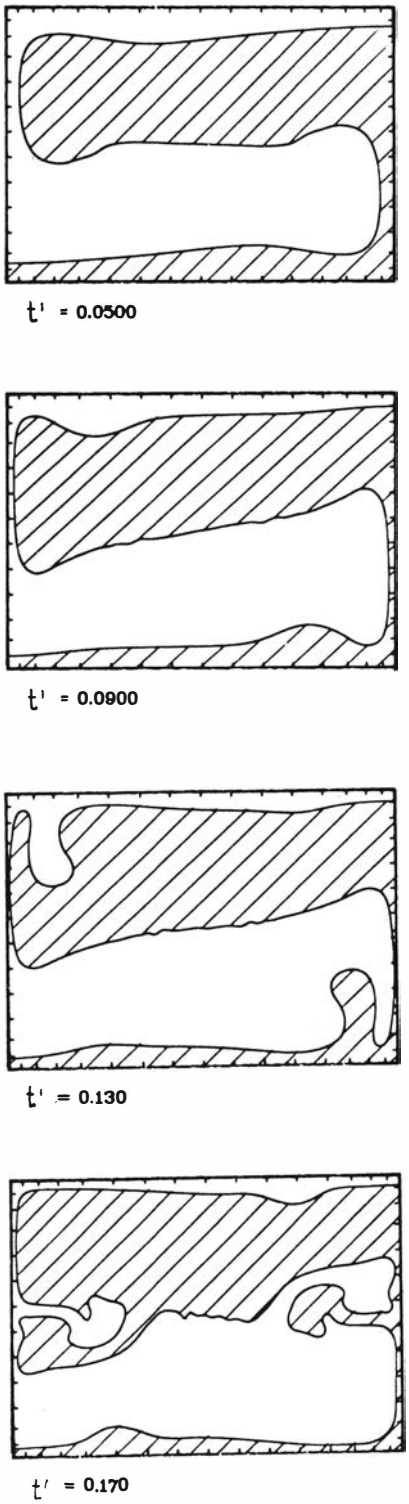

Fig. 10. Model with Ra= Rt=5 000 and no-slip condition at top and bottom. In other respects, like Fig. 9.

cation, as in the present models, gives a very effective mechanism to excite the oscillatory overstable mode (model 4 in Fig. 2 or 3).

As soon as Ra is sufficiently strong compared to Rt, multiple overturns lead to effective mixing. For the models 5 and 8 the nondimensional overturn time is of the order 0.1. With typical parameters of the lower crust (see section 1), this overturn time lies in the order of 1 Ma. Of course, the overturn time increases significantly as Ra is decreased.

Fig. 1 suggests that the flow will be in the single R.T.-regime if

$$Rt/Ra > 1/3 \tag{10}$$

(for Ra significatly larger than Ra_c). With the definitions of Ra and Rt (equ. 1 and 2) (10) reduces to

$$\frac{\Delta\varrho}{\varrho\alpha\Delta T} = \frac{\Delta\varrho}{\Delta\varrho_{th}} > 1/3 \tag{11}$$

where $\Delta\varrho_{th}$ is the maximum density contrast induced by thermal expansion. Thus, the parameters $\Delta\varrho$, $\Delta\varrho_{th}$ mainly determine whether convection or R.T.-overturns will occur, while the remaining parameters, g, h, $\varkappa$, η influence Ra and Rt in the same way, leaving the ratio Rt/Ra constant.

No-slip condition

The free slip boundary conditions in the previous models are rather idealized. More complicated structures develop if one chooses no-slip boundary conditions. Since a systematic series of no-slip models is not yet completed, the following models are shown only to illustrate the possible effects. Fig. 8 shows steady state convection with Ra=10 000 and no-slip conditions at the top and bottom. The volume originally situated in the lower half of the model is hatched. The interface is passively driven by the convective flow. Comparison with free slip convection (Fig. 3e) shows that the convective core now deforms in a non-uniform way. However, a test with aspect ratio 1, which is not shown here, leads to a convective core without shearing structures (a rigid body rotation). If Rt is increased, oscillatory behaviour after one overturn is observed for the combination Ra=7 500, Rt=2 500 (Fig. 9); however, the structure is complicated by secondary diapirs. In the case Ra=Rt=5 000 (Fig. 10), the secondary diapir forms so close to the stem of the primary diapir that it is swept upwards together with its own stem.

Effect of R.T.-overturns on the temperature field

From Figs. 5 and 6 it becomes obvious that an R. T.-overturn influences the temperature field or surface heat flux significantly if Rt exceeds a few hundred. If inverted density stratifications of the order of $\Delta\varrho$ = 100 kg m^{-3} occur in the lower crust (which may be due to partial melting), Rt will exceed a few hundred if the effective viscosity is less than or equal to around 10^{19} Pa · s (assuming h=15 km, $\varkappa 10^{-6} m^2 s^{-1}$). Of course, this is only an order of magnitude estimate because the rheology in nature is highly temperature dependent, prohibiting a direct application of the presented models. As a consequence of a high Rt, the arrival of a diapir should be seen as a surface heat flow anomaly, which, at very high Rt (Rt>3 000), should still be observable long after the time of emplacement. Thus, from the presence or absence of heat flow anomalies around recently emplaced diapirs, information about Rt and η can be inferred.

For salt diapirs, the above reasoning is complicated by the fact that the thermal conductivity of salt is about 2−3 times larger than that of other sedimentary rocks. This may lead to a long term anomaly of the surface heat flow of the same order due to conduction alone. This effect may be difficult to separate from an advective increase of the heat flow during emplacemnt of a salt diapir. Significant Rt-numbers during salt diapirism will occur if the effective viscosity during overturn is less than $\sim 10^{19}$ Pa · s (assuming $\Delta\varrho$ = 300 kg m^{-3}, h=10 km, $\varkappa = 2 \cdot 10^{-6} m^2 s^{-1}$).

Conclusion

In the preliminary series of models, the superposition of convection with a Rayleigh-Taylor instability was numerically investigated up to Ra and Rt values of 30 000 and 10 000 respectively. Flows of this kind can be important in the lower continental crust of regions subjected to anomalous heat flow from the mantle. Further cases of application are salt diapirs which may advect heat during their ascent. Ra, Rt space can be divided into a R.T.-regime (one overturn), an oscillatory regime (oscillations of the interface after one overturn) and a convective regime (multiple overturns). For a pure R.T.-overturn, the Rt-number provides a useful measure of how strongly initially horizontal isotherms are distorted, and of how strongly the surface heat flow will increase during and after the overturn.

The application to realistic situations is limited due to the idealized assumption of a constant viscosity. Actual crustal rheology is very complex, changing from brittle to ductile, and exhibits a stong temperature and stress dependence. Further improvments of the models will involve different thicknesses of the lighter source layers, which may lead to interesting effects if the dominant wavelength of the convective instability differs significantly from that of the R.T.-instability.

Acknowledgements. − I greatly thank U. Christensen who kindly provided the numerical code. Thanks are to Chris Talbot, P. Olson and H. Neugebauer for the stimulating discussions, and to H. Gadau and S. Stuhlert for processing the words.

REFERENCES

Christensen, U., 1984a: Convection with pressure- and temperature-dependent non-Newtonian rheology, Geophys. J.R. astr. Soc., *77*, 343−384.

Christensen, U., 1984b: Instability of a hot boundary layer and initiation of thermo-chemical plumes, Annales Geophysicae, *2*, 311−320.

Christensen, U., and D.A. Yuen, 1984: The interaction of a subducting lithospheric slab with a chemical or phase boundary, J. Geophys. Res., *89*, 4389−4402.

Jackson, M.P.A., and C.J. Talbot, 1986: External shapes, strain rates, and dynamics of salt structures, Geol. Soc. Am. Bull., *97*, 305−325.

Kirby, S.H., 1983: Rheology of the lithosphere, Rev. Geophys. Space Phys., *21*, 1458−1487.

Marsh, B.D., 1982: On the mechanism of igneous diapirism, stoping, and zone melting, Am. J. Sci., *282*, 808−855.

Neugebauer, H.J., and C. Reuther, 1986: Intrusion of igneous rocks − physical aspects −, Geol. Rundschau, *76*, 89−99.

Ramberg, H., 1981: Gravity, Deformation and the Earth's Crust in Theory, Experiments and Geologic Application, Academic Press, London, 2nd ed., 452 pp.

Richter, F.M., and C.E. Johnson, 1974: Stability of a chemically layered mantle, J. Geophys. Res., *79*, 1635−1639.

Schmeling, H., 1987: On the relation between initial conditions and late stages of Rayleigh-Taylor instabilities, Tectonophysics, *133*, 65−80.

Schmeling, H., and W.R. Jacoby, 1981: On modelling the lithosphere in mantle convection with non-linear rheology, J. Geophys. *50*, 89−100.

Schmeling, H., A.R. Cruden, and G. Marquart, 1988: Progressive deformation in and around a fluid sphere moving through a viscous medium: implications for diapiric ascent. Tectonophysics, 149, 17−34.

Stengel, K.C., D.S. Oliver, and J.R. Booker, 1982: Onset of convection in a variable-viscosity fluid, J. Fluid Mech., *120*, 411−431.

Weijermars, R., and H. Schmeling, 1986: Scaling of Newtonian and non-Newtonian fluid dynamics without inertia for quantitative modelling of rock flow due to gravity (including the concept of rheological similarity), Phys. Earth Planet. Int., *43*, 316−330.

Woidt, W.D., 1978: Finite element calculations applied to salt dome analysis, Tectonophysics, *50*, 369−386.

Printed by Ekenäs Tryckeri Ab, Ekenäs, Finland December 30th, 1988